RSC Advances

PAPER

View Article Online
View Journal | View Issue

Cite this: *RSC Adv.*, 2025, **15**, 5876

Functional modification and antibacterial evaluation of orthodontic adhesives with poly (lysine)-derived carbon dots

Linlin Xu,[a] Qianqian Zhang,[b] Yongzhi Xu,[b] Xuecheng Xu,[b] Mingchang Hu,[a] Jidong Xu,[c] Yu Song*[b] and Yuanping Hao *[b]

Received 11th December 2024
Accepted 11th February 2025

DOI: 10.1039/d4ra08710k

rsc.li/rsc-advances

Fixed appliances used in orthodontic treatment make oral hygiene difficult to maintain, leading to bacterial adhesion around brackets and consequently resulting in white spot lesions (WSLs). After the bracket debonding, the residual adhesive is difficult to remove precisely due to its appearance similar to tooth enamel. In this study, we successfully synthesized small-sized and highly active PL-CDs by one-pot pyrolysis using ε-poly-L-lysine as a precursor. It was incorporated into orthodontic adhesives for multi-function modification. Based on our experimental results, the 3 wt% PL-CDs modified orthodontic adhesive exhibited excellent antibacterial properties and color identifiability. The addition of 3 wt% PL-CDs did not affect the biocompatibility and mechanical properties of the adhesive, and the cell survival rate was up to 80%. Therefore, this study provides a new strategy to solve the two major problems of enamel white spot and adhesive removal in the process of fixed orthodontics, and has important clinical application.

1. Introduction

In clinical work, many patients with malocclusion are treated with orthodontic treatment to improve occlusion and aesthetic problems, and fixed orthodontic appliances are widely used because of their high efficiency and precise control of tooth movement.[1,2] Wearing fixed orthodontic appliances provides favorable conditions for bacterial colonization and plaque formation, and the metabolism of colonized bacteria produces acid, leading to tooth demineralization, clinically known as enamel "white spot lesions" (WSLs).[3,4] WSLs are one of the most common and problematic complications in orthodontic treatment.[5] Therefore, improving the antimicrobial properties of fixed orthodontic appliances is essential and has been the focus of orthodontic research.

The orthodontic adhesive is an important part of the bonding interface between brackets and the tooth surfaces, and studies have shown that plaque is more likely to accumulate at the bonding interface relative to the bracket surface.[6] Therefore, the antimicrobial modification of adhesives is of great clinical importance for the prevention of WSLs. In recent years, nanomaterials have been widely used in dentistry due to their structural stability and excellent antimicrobial properties,[7,8] and the study of nanomaterial-based antimicrobial agents for modification of orthodontic adhesives has also received increasing attention.[9–14] Sodger *et al.* studied the introduction of TiO_2 nanoparticles into orthodontic adhesives, and the results confirmed that the doping of TiO_2 nanofillers (1% w/w) could improve the antimicrobial properties of orthodontic adhesives without affecting the adhesive bonding.[15] Some scholars introduced ZnO quantum dots (ZnQDs) into orthodontic adhesives, and the results showed that ZnQDs-doped orthodontic adhesives had good antimicrobial properties and biocompatibility. Currently. The most researched is the introduction of Ag NPs as fillers into orthodontic adhesives to enhance their antimicrobial properties.[16] However, the addition of Ag NPs changed the color of orthodontic adhesives to dark grey, which could not meet the aesthetic demand of orthodontics,[17] and agglomeration occurred, affecting the physical properties of the adhesives.[18] Current research on nanofillers mainly focuses on metal nanoparticles, and the systemic toxicity and safety of nanoparticles due to release and ingestion still need to attract attention and further research.[19,20]

In addition, to address the clinical difficulty in distinguishing orthodontic adhesives from enamel, researchers have now explored methods for visual identification and removal of adhesives, such as dental microscope assistance,[21] selective staining of adhesives,[22,23] temperature-sensitive discoloration of adhesives,[24] and fluorescence-assisted identification.[25,26] However, all the above methods have different degrees of problems in practical application, such as the need to resort to special expensive equipment and poor adaptability. Therefore, modifying orthodontic adhesives to be distinguishable may be

[a]School of Stomatology of Qingdao University, Qingdao 266003, China
[b]Qingdao Stomatological Hospital Affiliated to Qingdao University, Qingdao 266001, China. E-mail: bmusy2002sy@163.com; yphao@qdu.edu.cn; Tel: +8616622380102
[c]Qingdao Jiaozhou Central Hospital, Qingdao 266300, China

an effective way to help clinicians precisely remove adhesives and protect enamel in some cases.

Carbon dots (CDs), as novel carbon-based biomaterials with unique optical properties, excellent biocompatibility, and accessible surface modification, have great potential for antimicrobial infections.[27–30] CDs precursors come from a wide range of sources, including chemical small molecules, polymers, various plants, and other types of materials, but only a small fraction of precursor-derived carbon dots have antimicrobial properties.[31] Biomass-derived CDs can meet the needs of large-scale production and have the advantage of sustainable development, but the synthetic pathway of CDs,[32–34] the complex reactions during synthesis, and the structure of the final CDs still need to be further investigated; drug-derived CDs exhibit highly efficient antimicrobial properties, but the mechanisms of their induced bacterial resistance and inactivation need to be explored in depth.[32–34] Poly-lysine-derived CDs (PL-CDs) have been shown to have good bactericidal activity. PL-CDs do not require additional modifications and special groups, and highly antibacterial CDs can be obtained by direct precursor carbonization; the amino group of the precursor is retained on the surface of the CDs, which enhances adhesion to negatively charged bacterial membranes, and it is well biocompatible. Some studies have used PL-CDs crosslinked with oxidized dextran to construct an injectable hydrogel, which exhibits high efficiency against *S. aureus*.[35] Nonetheless, there are relatively few studies on the application of CDs in dentistry.

Our group used PL-CDs as root canal disinfectants against periapical infections caused by *Enterococcus faecalis* in a previous study.[36] CDs kill bacteria through multiple antibacterial mechanism.[37–39] We hypothesized that PL-CDs-modified orthodontic adhesives may play a role in preventing WSLs (Scheme 1). Firstly, PL-CDs were synthesized by one-pot pyrolysis and their morphology was observed by high-resolution transmission electron microscopy, as well as their spectra, zeta potential, and elemental compositions were also investigated. The antimicrobial properties of PL-CDs were verified by agar diffusion test and bacterial morphology observation. They were introduced into orthodontic adhesives and their antimicrobial activity against free bacteria by CFU and SEM, and their destructive properties against bacterial biofilms were assessed by crystal violet staining as well as live/dead assay. Finally, the biocompatibility and physical properties of PL-CDs-modified orthodontic adhesives were tested to provide experimental support for their clinical applications.

2. Materials and methods

2.1. Materials

ε-Poly-L-lysine (PL) (MW ∼ 4000) was purchased from Dipper Chemical Technology Co., Ltd (Shanghai, China). Live/dead Bacterial Staining Kit, Live/dead Cell Staining Kit, phosphate buffered saline (PBS, pH 7.4), Dulbecco's modified Eagle's medium (DMEM), Brain–Heart Infusion Broth (BHI), and Agar and Lysogeny Broth (LB) were purchased from Solarmbio Science & Technology Co., Ltd (Beijing, China). Fetal bovine serum (FBS), penicillin–streptomycin, and Cell Counting Kit-8 (CCK-8) were provided by Wuhan Pricella Biotechnology Co., Ltd (Wuhan, China). All reagents were used directly without further purification.

2.2. Preparation and characterization of PL-CDs

PL-CDs were synthesized by one-pot pyrolysis.[36] In brief, 1 g of PL in a corundum crucible was heated in a box muffle furnace at 240 °C for 3 h. After the furnace chamber cooled naturally to room temperature, the residue was ground into powder and dissolved in 20 mL of deionized water. The mixture was sonicated for 60 min, centrifuged (11 000 rpm) for 30 min, and finally the supernatant was dialyzed with deionized water for 24 h and lyophilized (Alpha1-2 LD plus; Christ®, Germany). The PL-CDs were stored at 4 °C for further use.

The micromorphology and size of PL-CDs were characterized using high-resolution transmission electron microscopy at an accelerating voltage of 100 kV (HRTEM, JEM-2100F, Japan). One hundred nanoparticles were randomly selected from the TEM images. The size distribution was determined using ImageJ software. The composition of PL-CDs powders was detected by X-ray photoelectron spectroscopy (XPS), and the results were

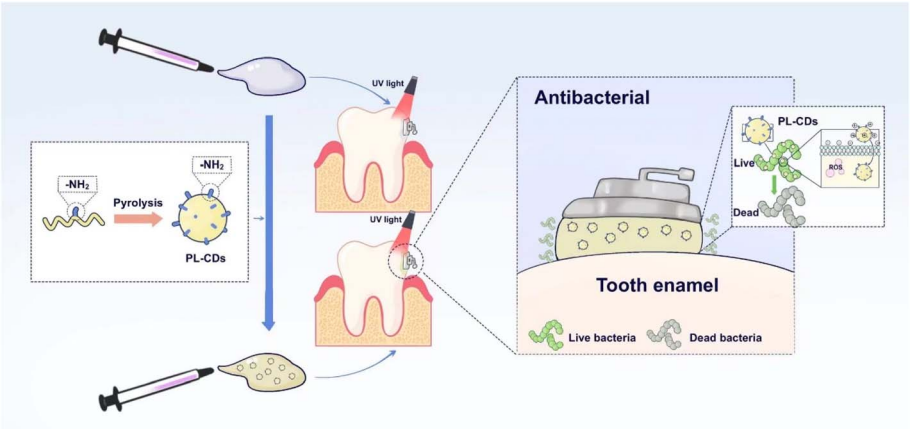

Scheme 1 Schematic illustration of PL-CDs modified orthodontic adhesives for preventing WSLs.

processed using the AVANTGE program. The PL and PL-CDs were dispersed in deionized water at the same concentration (400 μg mL^{-1}), with pH values of 5.27 and 5.39, respectively. Their zeta potential was obtained at 25 °C using the instrument zeta sizer (Nano ZSE, UK). Ultraviolet-visible spectrophotometry (UV-vis) absorption spectra were detected using a UV-8000 spectro-meter (Yuanxi, Shanghai, China).

2.3. Preparation of resin sheet discs for modified orthodontic adhesives

Commercial orthodontic adhesive (3M™ Transbond™ XT Light Cure Adhesive, 3M, UK) was used as the adhesive matrix. The PL-CDs were homogeneously mixed into the adhesive using a plastic mixing spatula under darkroom conditions to obtain the PL-CDs-modified orthodontic adhesive. In the following, we will refer to the PL-CDs-modified orthodontic adhesive as Tb-XT. The mixing ratios were 1 wt% (Tb-XT1), 2 wt% (Tb-XT2), and 3 wt% (Tb-XT3), using 3M™ Transbond™ XT Light Cure Adhesive without any filler added as a control (0 wt%, Tb-XT0). The lids of the 96-well plates were used as molds, and the adhesives were filled into the lids individually. Then, the pre-prepared glass plates were squeezed firmly, scraped off the excess adhesives, and cured through the light curing unit for 60 s on each side for complete curing to obtain orthodontic adhesive resin sheet discs of approximately 8 mm in diameter and 1 mm in thickness. The cured resin sheets were removed, ground, and polished with a low-speed head. The samples were magnetically stirred in distilled water at 100 rpm for 1 h to remove uncured monomers. The specimens were fumigated in a 75% ethanol fumigator for 3 h and irradiated with UV light on both sides for 30 min before use.

2.4. Agar diffusion assay

Streptococcus mutans (*S. mutans*, ATCC25175) were purchased from Shanghai Biology Collection Center, China. The strains were expanded in a 37 °C shaker for 12 h. A suspension of *S. mutans* with a colony count of 1×10^7 colony forming units (CFU) mL^{-1} was spread evenly on BHI nutrient agar plate medium with a cotton swab. After punching with a 200 μL tip, 100 μL of different concentrations of PL-CDs suspension was added and incubated at 37 °C for 24 h in a constant temperature incubator. The diameter of the circle of inhibition was measured three times in different directions with a vernier caliper, and the average value was taken as the diameter of the circle of inhibition of the sample. The experiment was repeated three times with three independent replications.

2.5. Antimicrobial evaluation of colony-forming units

S. mutans and *Escherichia coli* (*E. coli*, BNCC 133264, BeNa Culture Collection, China) were chosen as typical Gram-positive bacteria and Gram-negative bacteria used in antibacterial assay, respectively. For example, after co-culturing the pre-prepared resin sheet discs with *S. mutans* solution (1 mL, 1×10^7 CFU mL^{-1}) for 12 h. The bacterial solution collected after co-cultivation was serially diluted, and 20 μL of the diluted bacterial solution was inoculated onto BHI solid agar medium. The number of *S. mutans* colonies was counted to calculate the bactericidal rate.

$$\text{Bactericidal rate}(\%) = \frac{(\text{Control CFU} - \text{Treatmeat CFU})}{\text{Control CFU}} \times 100\%$$

2.6. Bacterial micromorphology and distribution observation

After the above co-culture, the resin discs were washed three times with PBS for three minutes each time, then fixed with 2.5% glutaraldehyde, dehydrated with 30%, 50%, 70%, 80%, and 100% alcohol for 10 min each time, and then dried with supercritical CO_2 after isoamyl acetate replacement. The bacterial distribution and bacterial morphology of the resin sheet discs were observed after spraying the gold coating for 2 min, and then viewed under an accelerating voltage of 100 kV using a scanning electron microscope (SEM, Zeiss, Germany).

2.7. Anti-biofilm experiment

S. mutans suspension (1×10^7 CFU mL^{-1}) was added to the 24-well plate and incubated at 37 °C. After 24 h, the *S. mutans* biofilm was collected by rinsing with PBS (pH 7.4) very gently to remove planktonic bacteria. Then the pre-prepared resin sheets were co-cultured with the obtained biofilm for 24 h. After that, the biofilm was stained by 0.1% crystal violet staining solution and LIVE/DEAD™ BacLight™ Bacterial Viability Kit (Solarbio, China) following the manufacturer's protocol, respectively. 30 min later, 95% ethanol was used to dissolve the biofilm for the crystal violet staining assay, then diluted and transferred to 96-well plates. The absorbance value of each well at 570 nm was measured with a microplate reader (Bio-TEK, USA), and the biofilm destruction rate was calculated as follows:

$$\text{Destruction rate}(\%) = \frac{\text{Control OD} - \text{Treatmeat OD}}{\text{Control OD}} \times 100\%$$

For the live/dead assay, the confocal microscopy images of stained bacteria were performed on a laser scanning confocal microscope (SP8, Leica Microsystems). Nuc Green is a green nucleic acid dye that appears green for bacteria with intact cell membranes, and the red nucleic acid dye EthD-III stains only dead bacteria with damaged cell membranes.

2.8. Biocompatibility test

2.8.1. Hemolysis assay. 1 mL of anticoagulated blood was taken from healthy rats (purchased from Pengyue Experimental Animal Breeding Center in Jinan City, China) and diluted with 0.9% saline (5 mL). The diluted blood solution (50 μL) was then added to EP tubes containing different concentrations of leachate (1 mL), ultrapure water (positive control), and 0.9% saline (negative control), respectively. The mixtures were incubated at 37 °C for 1 h. The mixtures were centrifuged at 5000 rpm for 5 min, and the absorbance of the supernatant at 540 nm was measured using an enzyme marker (PowerWave X,

BioTek). The experiment was repeated three times. The hemolysis rate (Haemolysis %) was calculated as follows:

$$\text{Haemolysis rate}(\%) = \frac{\text{Abs} - \text{Abs}(-)}{\text{Abs}(+) - \text{Abs}(-)} \times 100\%$$

2.8.2. CCK-8. Each set of resin sheet discs was incubated in 5 mL of Dulbecco's Modified Eagle Medium (DMEM, Solarbio, Beijing) and 10% FBS at 37 °C, 5% CO_2 for 24 h to obtain the extracts. Mouse fibroblast cell line (L929) was obtained from the Cell Culture Center, Shanghai Institute of Life Sciences, Chinese Academy of Sciences, (Shanghai, China). L929 cells were inoculated into 96-well plates at 3×10^3 cells per well and incubated at 37 °C, 5% CO_2 for 24 h. After removing the medium and washing with PBS, the extracts were dropped into 96-well plates separately, and the cells with the pure medium were used as the control group. On days 1, 3, and 5 of the cell culture, 10% CCK-8 solution (CCK-8 kit, Procell, China) was added to each well after washing with PBS and incubated for another 2 h to assess cell activity. The absorbance at 450 nm was measured using a microplate reader (Bio-TEK, USA). The absorbance of each culture well was averaged from five replicates.

2.8.3. LIVE/DEAD cell staining. L929 cells were inoculated in confocal Petri dishes at 5×10^3 per well and cultured at 37 °C, 5% CO_2 for 24 h. After removing the medium and washing with PBS, the extracts from different groups were added to the confocal Petri dishes and cocultured with the cells separately. After 48 h, the cells were washed with PBS, and subsequently stained using live/dead cell staining reagents according to the workbook. After 30 min, the distribution of live and dead cells was visualized under a laser confocal microscope.

2.9. Shear strength and residual index tests on isolated teeth

Forty human maxillary first premolar teeth extracted for orthodontic reasons were obtained from Qingdao Stomatological Hospital and approval was provided by the Ethics Committee of Qingdao Stomatological Hospital (2023KQYX038). Inclusion criteria were premolar teeth that were free of caries, cracks, demineralization, or abrasions and had not received dental treatment. The teeth were selected and randomly divided into four groups ($n = 10$). The premolar teeth were vertically encased in epoxy resin to ensure that the tooth surface of the enamel was perpendicular to the epoxy resin base. After cleaning the crowns with fluoride-free toothpaste, all teeth were acid etched with 37% phosphoric acid gel for 30 s, rinsed with deionized water, and blown dry with an air gun. The primer (3M™ Transbond™ XT Light Cure Primer, 3M, UK) was applied in thin coats to the enamel surface, and the adhesive paste was placed at the base of the brackets and bonded to the center of the clinical crown on the tooth surface. After removing the excess adhesive around the brackets, the adhesive between the base of the brackets and the enamel was polymerized using a light-curing lamp (Kerr, US) from the proximal-central and distal-central directions for 30 s. The shear bond test was performed after 24 h to evaluate the bond strength of each group. The bottom area of the bracket mesh was approximately 12.97 mm^2, and the bond strength was calculated according to the following formula:

$$\text{Bond strength}(\text{MPa}) = \frac{\text{maximum load}(\text{N})}{\text{bottom area of bracket mesh}(\text{mm}^2)}$$

The enamel surface of each sample was viewed through a stereomicroscope for residual index analysis after debonding. The following categories were used for the Adhesive Residue Index (ARI) analysis:

- 0 = no adhesive residue on the enamel;
- 1 = less than half of the adhesive residue on the enamel;
- 2 = more than half of the adhesive residue on the enamel;
- 3 = all of the adhesive residue on the enamel.

2.10. Statistical analysis

All data were presented as mean values ± standard deviation based on experiments in triplicate. A one-way analysis of variance and a *t*-test were used to analyze the differences between the experimental groups. Statistical analyses were performed using GraphPad PRISM 9.5, and the significant differences in the data were indicated by $*p < 0.05$, $**p < 0.01$ and $***p < 0.001$.

3. Results

3.1. Preparation and characterization of PL-CDs

PL-CDs were successfully synthesized using a one-pot pyrolysis method. The prepared PL-CDs were demonstrated to be homogeneous spherical particles with smooth surfaces and good dispersion by high-resolution transmission electron microscopy. The average diameter of PL-CDs was 3.06 ± 0.83 nm (Fig. 1a and b). The UV-visible absorption spectrum of PL-CDs is shown in Fig. 1c. The peak at 280 nm was attributed to the typical π–π* leaps of the aromatic sp^2 structural domain (C=C). In contrast, the shoulder peak at 300–400 nm corresponds to the n–π* leaps of the C=O and C–N bonds,[40,41] and the results confirm the successful synthesis of the PL-CDs. The uniformly dispersed suspension of PL-CDs was shown as a pale yellow and blue color under sunlight and UV light (365 nm), respectively. The elemental composition of the PL-CDs probed by XPS was mainly composed of carbon, nitrogen, and oxygen. As shown in Fig. 1d and e, The C 1s spectra of PL-CDs were observed to display three types of carbon bonds: C–C (284.8 eV, 77.85%), C–O (286.3 eV, 13.9%), and C=O (288.09 eV, 8.25%) correspond to sp^3. The O 1s spectra were observed to show two types of oxygen bonds: C=O (531.7 eV, 78.15%) and C–O (533.29 eV, 21.85%). The N 1s spectra were observed to show three types of nitrogen bonds: $-NH_2$ (401.08 eV, 68.29%), C–N (399.48 eV, 25.25%), and C=N (398.17 eV, 6.46%). In addition, the zeta potential results showed that the charged nature of precursor PL was not significantly different from that of PL-CDs (Fig. 1f), which showed high positive charge characteristics, confirming the presence of primary amines on the surface of PL-CDs.

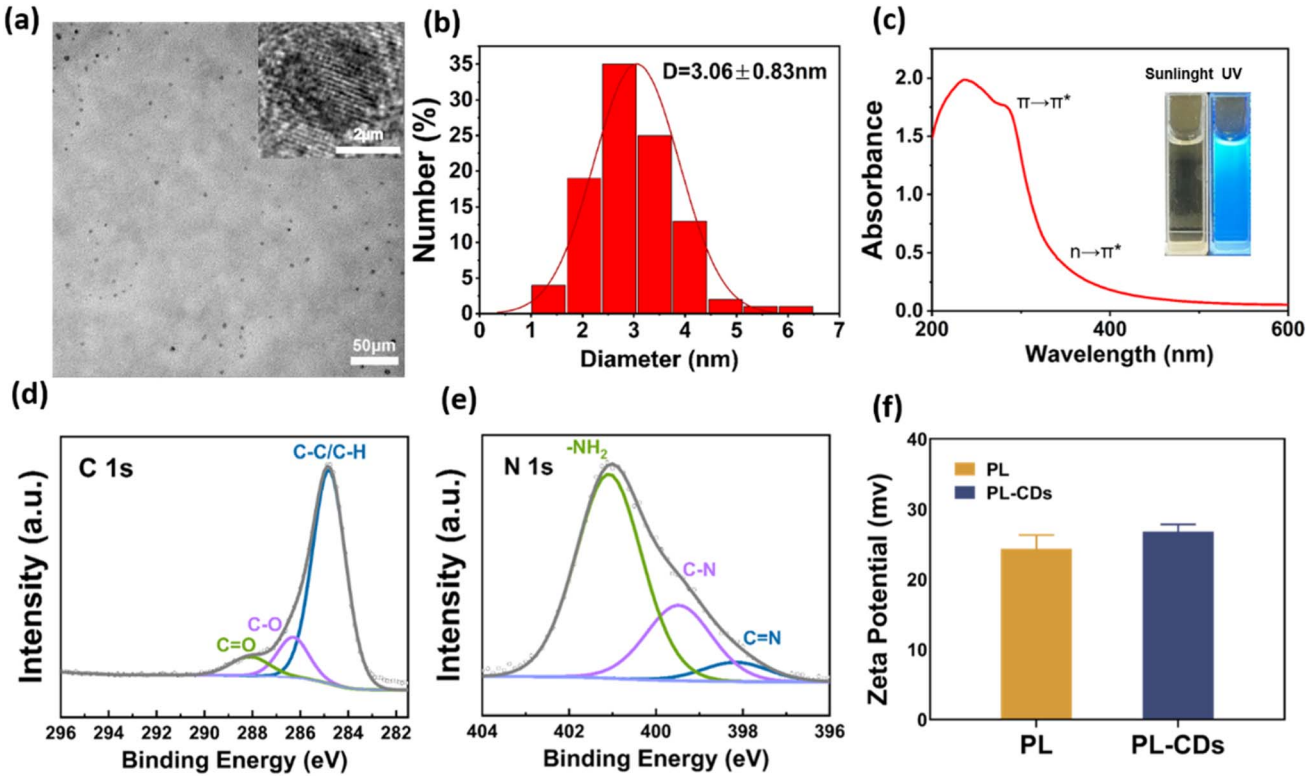

Fig. 1 (a) TEM and HRTEM images of Pl-CDs. (b) Particle size distribution map of PL-CDs. (c) UV-vis absorption spectra of PL-CDs. The inset is a photograph of the PL-CDs solution under sunlight and UV. (d) XPS C 1s spectra of PL-CDs. (e) XPS N 1s spectra of PL-CDs. (f) Zeta potential of PL and PL-CDs.

3.2. Antimicrobial performance of PL-CDs

The agar diffusion method was used to verify the antimicrobial performance of PL-CDs using *S. mutans* as typical Gram-positive bacteria. As shown in Fig. 2a, there are no antibacterial rings in the control group. Notably, the antibacterial ring gradually increased with the gradient addition of PL-CDs, and the antibacterial effect showed a concentration dependence. Significant differences in the antibacterial ring diameters among the groups confirmed the good antibacterial performance of our synthesized PL-CDs. The SEM images of bacteria treated with PL-CDs suspension showed multiple irregular ruptures, cytoplasmic efflux, swelling enlargement, and a multi-point disrupted morphology as shown in Fig. 2c and d. In contrast, the untreated bacteria showed an intact morphology and a smooth surface.[36]

3.3. Antimicrobial properties of PL-CDs modified orthodontic adhesive

PL-CDs, which have been shown to have significant antimicrobial activity as described above, were added to orthodontic adhesives. *S. mutans* and *E. coli* were chosen as typical Gram-positive as well as Gram-negative bacteria, and the antimicrobial activity of modified orthodontic adhesives was verified using plate counting method. The results in Fig. 3b and c showed that the modified orthodontic adhesives had good antibacterial effects on both *S. mutans* and *E. coli*. It showed a concentration-dependent effect. The antimicrobial rates of all three groups showed significantly differed from the control group, especially the antimicrobial rate was close to 100% in the Tb-XT3 group. Furthermore, the orthodontic adhesives resin model co-cultured with bacteria was observed under SEM. As shown in Fig. 3d, many bacteria with a regular bacterial morphology and a smooth surface were distributed on the surface of the orthodontic adhesives in the blank group. On the contrary, the number of bacteria adhering to the resin sheets containing PL-CDs was significantly decreased, and the bacterial morphology was severely disrupted.

3.4. Anti-biofilm properties of PL-CDs modified orthodontic adhesive

S. mutans is one of the main pathogens of caries, which can adhere to enamel and other bacterial surfaces,[42] colonise and form bacterial biofilms in the oral cavity, while producing organic acids that promote enamel demineralisation[43] and thus lead to dental caries.[44] Therefore, *S. mutans* as a model bacterium was chosen to evaluate the biofilm resistance of the modified adhesive by live bacterial staining and crystal violet staining. Crystalline violet staining of the biofilm images was shown in Fig. 4b. The control group exhibited very intact and homogeneous biofilms, whereas the experimental group was seen to have different degrees of destructive effects on bacterial biofilms. Among them, the biofilm destruction was obvious in

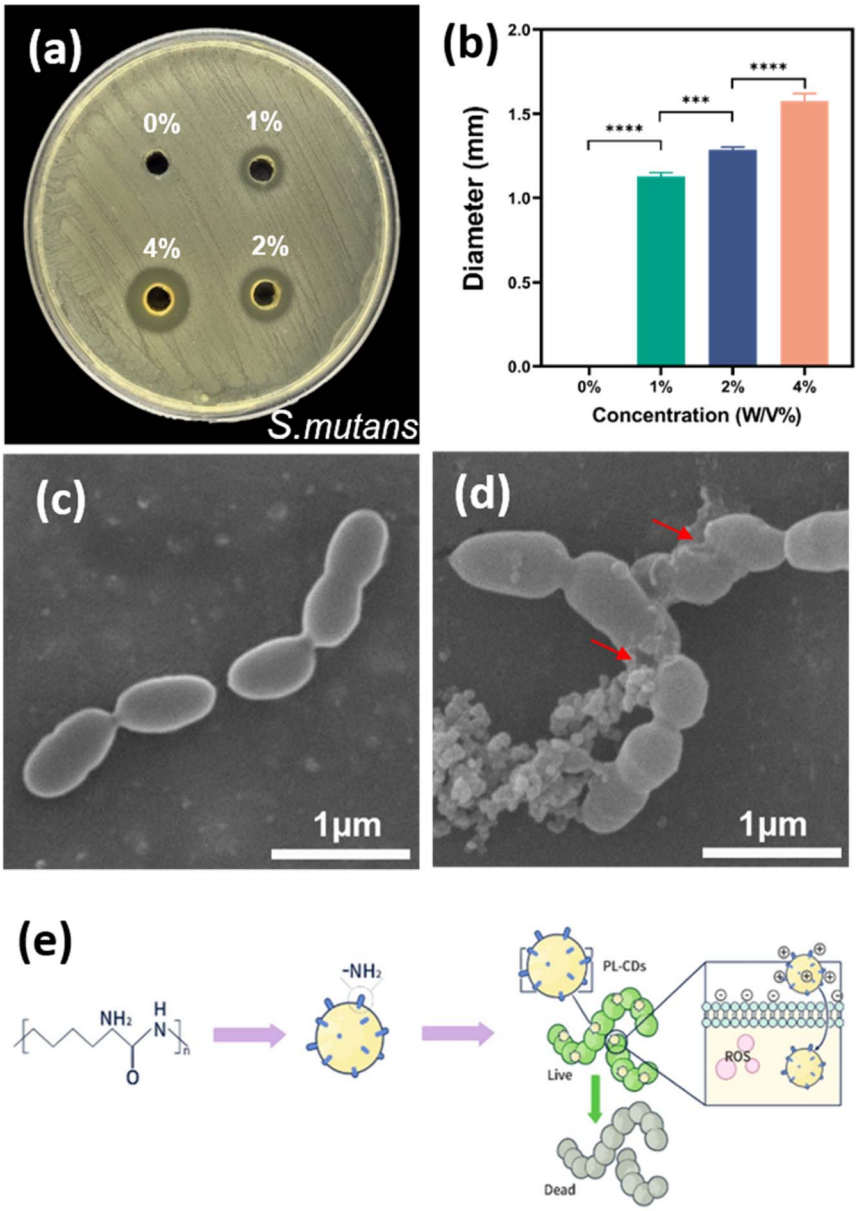

Fig. 2 (a) Image of antimicrobial rings with different concentrations of PL-CDs. (b) Assessment of the antimicrobial ring diameters at different concentrations of PL-CDs. (c) SEM images of *S. mutans* before co-culture with PL-CDs modified orthodontic adhesive and (d) bacteria after co-culture. Arrowheads indicate damaged cell membranes. (e) Schematic diagram of the antimicrobial mechanism of PL-CDs.

the Tb-XT3 group, and the biofilm turned thin and loose. Although the biofilm destruction could be observed in the Tb-XT1 and Tb-XT2 groups, the destruction was not obvious due to the small concentration of PL-CDs and the thicker bacterial biofilm. Notably, the damage in the contact region of the orthodontic adhesive specimen was obvious and significant compared with the other regions, indicating that PL-CDs-modified orthodontic adhesive mainly exhibits a contact antibacterial.

The fluorescence images of the biofilm were observed using laser confocal. As shown in Fig. 4d, the control biofilm was dense and uniform. A large amount of green fluorescence was visible. The experimental group showed a significant destruction effect on the biofilm with the concentration increased. Although Tb-XT1 had a certain destructive effect on the biofilm, much green fluorescence was still visible. The biofilm receiving Tb-XT3 treatment demonstrated significantly more red-stained bacteria than those receiving other treatments (Fig. 4d), suggesting the damage of cell membrane.

3.5. Biocompatibility evaluation of PL-CDs modified orthodontic adhesives

Haemocompatibility is one of the main criteria for the success of the clinical application of nanomaterials. As shown in Fig. 5a, the supernatants of the modified orthodontic adhesives were clear and transparent after interaction with blood. The

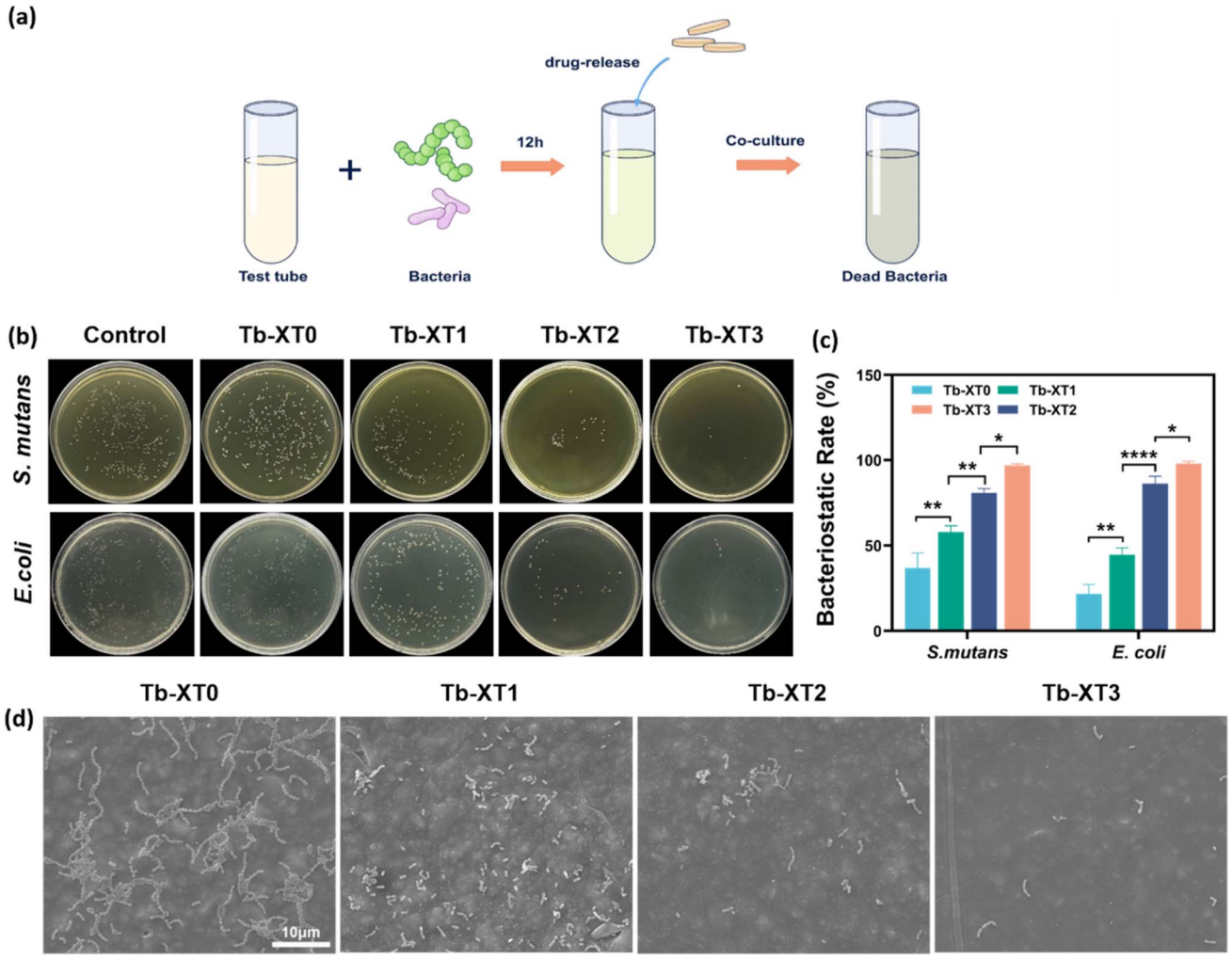

Fig. 3 (a) Schematic representation of the anti-*S. mutans* performance of PL-CDs-modified orthodontic adhesive. (b) *S. mutans* and *E. coli* on agar plates after treatment with PL-CDs-modified orthodontic adhesive. The concentrations were 1 wt% (Tb-XT1), 2 wt% (Tb-XT2), and 3 wt% (Tb-XT3) (c) inhibition rates of PL-CDs-modified orthodontic adhesive *for S. mutans* and *E. coli*. (d) SEM images of bacterial distribution on the surface of resin sheet discs.

haemolysis rates were all lower than 2%, and there was no significant difference with the negative control group. These results indicated that the prepared PL-CDs modified orthodontic adhesives had good haemocompatibility.

Subsequently, the cytocompatibility of PL-CDs modified orthodontic adhesives was assessed using the CCK-8 assay. The results were shown in Fig. 5b, the cell viability was higher than 80% in all groups, and there was no significant difference among Tb-XT1 and Tb-XT2 and the Tb-XT0 groups. The cytotoxicity of the modified orthodontic adhesives was further evaluated by a live/dead cell staining kit. Laser confocal images showed that after 48 h of co-culture, the cell density of each group decreased with the increase of PL-CDs (Fig. 5c), but there was no significant difference in the number and the morphology of viable cells among these groups. The laser confocal images were analyzed, and the results are illustrated (Fig. 5d). No significant differences were found among the groups, except between Tb-XT0 and Tb-XT3. The above experiments showed that the adhesive with the addition of PL-CDs still had good cytocompatibility.

3.6. Physical properties testing of orthodontic adhesives modified with PL-CDs

Modification of orthodontic adhesives should not affect the physical properties of orthodontic adhesives. Shear strength and bond residual index are important indicators to judge the physical properties of orthodontic adhesives, so we tested these two indicators by using a universal tension machine. As shown in Fig. 6b, there was no significant difference between Tb-XT0, Tb-XT1, and Tb-XT2. Compared with Tb-XT0, the bond strength of Tb-XT3 was slightly reduced, mainly due to the fact that with the increase in the addition of PL-CDs, the light scattering of the binder increases and the transparency decreases, which affects the degree of polymerisation of the resin during the light-curing process. However, the results proved that the minimum shear

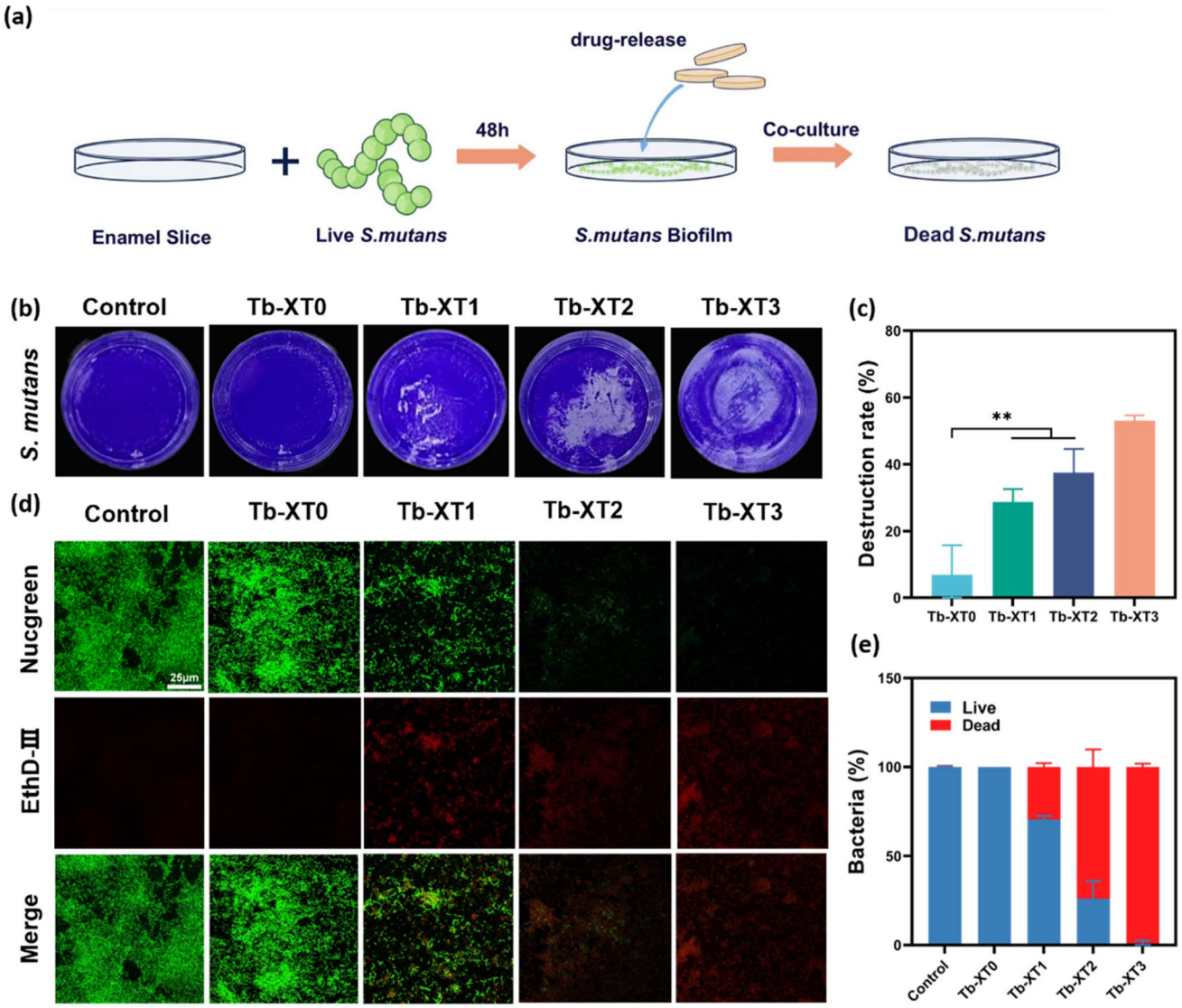

Fig. 4 (a) Schematic diagram of the anti-biofilm properties of PL-CDs-modified orthodontic adhesive. (b) Photographs of crystal violet biofilm destruction after treatment with different concentrations of PL-CDs-modified orthodontic adhesive. (c) Crystal violet biofilm destruction rate, $^{**}p < 0.01$. (d) Photographs of CLSM of *S. mutans* after 24 h incubation with different concentrations of PL-CDs-modified orthodontic adhesive treatments. Green (Nucgreen) and red (EthD-III) indicate live and dead bacteria, respectively. (e) Assessment of the percentage distribution of live and dead bacteria.

strength of Tb-XT3 remained above 8 MPa, which meets the clinical requirements for bond strength.[45]

The ARI index is an auxiliary index for evaluating the bonding effect of the adhesive to the enamel surface.[46] An ARI index larger than 2 indicates that bonding fracture mainly occurs at the bracket bonding interface, which causes less damage to the enamel; whereas an ARI index of less than 2 suggests that fracture mainly occurs between the enamel and the bonding agent, in which case the brackets may cause damage to the enamel during dislocation.[47] The shear strength experiments revealed a slight decrease in the shear strength of the adhesive with the addition of PL-CDs compared to the Tb-XT0 group, which may lead to debonding of the adhesive from the bracket or the tooth surface. The residual indicators were analysed and the results are shown in Fig. 6c, in which the gradient of PL-CDs increased the proportion of adhesive residue on the tooth surface after debonding, while the adhesive residue on the bracket was reduced, indicating that the adhesive residue after the addition of PL-CDs was mainly manifested in the bracket adhesive interface, which reduces the possibility of enamel damage in the process of bracket debonding.

In addition, the modified orthodontic adhesives had a slightly pale yellowish-brown color, which was distinctly different from the color of normal enamel, which was helpful in minimising the damage to enamel during bracket removal at the end of treatment in orthodontic clinical work. The above experiments not only ensured the bond strength of orthodontic brackets in orthodontic treatment, but also effectively reduced the risk of enamel damage during bracket removal.

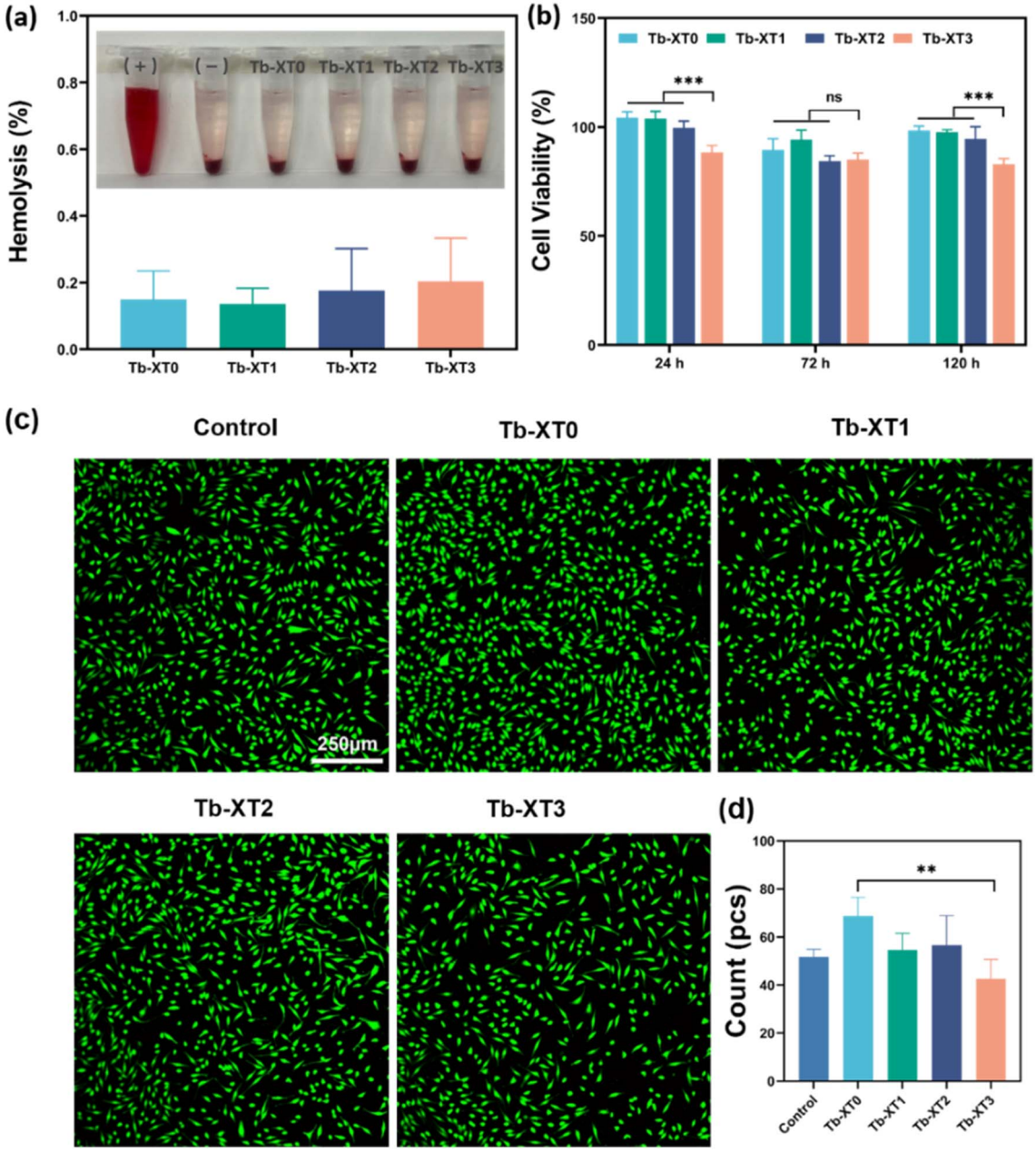

Fig. 5 (a) Hemolysis rate of erythrocytes treated with PL-CDs leach solution, and the inset is a photograph of erythrocytes after treatment with PL-CDs. (b) Cell viability of L929 after incubation with PL-CDs extract. (c) CLSM images of L929 after incubation with PL-CDs extract. (d) Assessment of the count of L929 in CLSM images.

4. Discussion

Fixed appliances used in orthodontic treatment make oral hygiene difficult to maintain, leading to bacterial adhesion around the brackets. After the bracket debonding, the residual adhesive is difficult to remove precisely due to its appearance similar to tooth enamel.[48–50] To address these issues, this study introduces PL-CDs as multifunctional modifiers into commercial adhesives for the first time, imparting antimicrobial properties and visually distinguishable colors. We chose PL as the precursor for antimicrobial carbon dots because PL is a lysine homopolymer consisting of lysine α -carbonyl and ε-amino groups bonded *via* amide bonds.[51] The potential antimicrobial mechanisms of PL mainly include:[52–54] (1) the cationic properties of PL can affect the integrity and permeability of microbial cell walls and cell membranes; (2) PL-induced stress inhibits the major metabolic pathways of microorganisms, mainly glycolysis and tricarboxylic acid cycle, leading to bacterial death. PL-CDs were obtained by using a one-pot pyrolysis method.[36] The particle size of PL-CDs is only about 3 nm, and its tiny particle size is easily absorbed by the bacteria, which interferes with the intracellular components of the bacteria and induces the death

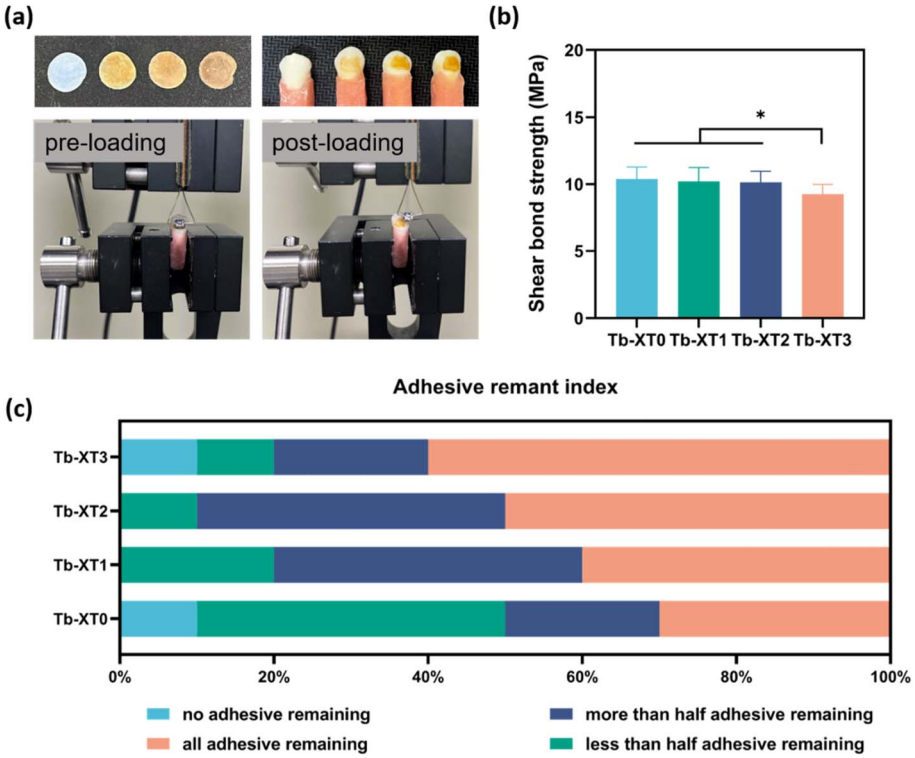

Fig. 6 (a) Schematic before and after loading of orthodontic adhesive shear strength test. The image inserted above is a color comparison of the resin sheet discs and the orthodontic adhesive on the tooth surface under natural light. (b) Shear strength of PL-CDs-modified orthodontic adhesive. (c) ARI: assessment of the adhesion residual index of PL-CDs-modified orthodontic adhesive.

of the bacteria.[55,56] Meanwhile, PL-CDs retained the high positive charge property of precursor PL, and this charge property can make PL-CDs easily adsorb negatively charged bacteria, inducing oxidative stress in the bacteria and destroying the structure of cell membranes and leading to the death of bacteria.[36,56–58] PL-CDs can also produce reactive oxygen species (ROS), which has been verified in our previous experiment using PL-CDs as root canal disinfectants to combat periapical periodontitis. A large amount of ROS can destroy bacterial protein and outer membrane to achieve the bactericidal effect.[36] Based on our experimental results, the antibacterial and color recognition properties of PL-CDs were demonstrated. In addition, the addition of 3 wt% PL-CDs did not affect the biocompatibility and mechanical properties of orthodontic adhesives.

The PL-CDs modified orthodontic adhesives possessed multiple antimicrobial modes of contact as well as release antimicrobials at the same time, and showed highly efficient resistance to planktonic bacteria and biofilms. SEM observation of the destruction and morphology of bacterial on the surface of PL-CDs-modified orthodontic adhesives also verified the destruction. The high antimicrobial performance of PL-CDs-modified orthodontic adhesives may be related to the aforementioned tiny particle size of PL-CDs and the high positive charge density on their surfaces.[31] Many studies on the modification of composite resin materials have focused only on whether the mechanical properties of the materials are affected, without the detection of toxicity.[59–61] The modification of adhesive by metal nanoparticles in the early stage has raised concerns about the potential toxicity of metal particles in the human body over the long term.[17,62] Although PL-CDs are different from metal nanoparticles, it is still necessary to assess biocompatibility as a new biomaterial. We performed tests such as live-dead cell staining to confirm that the modified orthodontic adhesives showed good biocompatibility, and the survival rates of cells was as high as 80%.

The ideal modified orthodontic adhesive should have sufficient enamel bonding strength to prevent bracket dislodgement during tooth movement and chewing in the course of orthodontic treatment. The addition of PL-CDs did not affect the properties of the original orthodontic adhesive, and the experiment proved that it could meet the need of bond strength in orthodontic clinic. One of the reasons may be that the high antibacterial properties of PL-CDs make it acceptable to add a small amount in orthodontic adhesives. However, orthodontic treatment is a long-term process, and further studies are needed to evaluate the long-term physical properties of PL-CDs-modified orthodontic adhesives in the oral environment. It is important to maintain the integrity of the enamel surface after bracket removal in orthodontic treatment. Due to the similarity in appearance between enamel and adhesive, it is difficult to identify and accurately remove the adhesive, and insufficient removal leads to bacterial adherence.[63,64] PL-CDs obtained after high-temperature pyrolysis of PL is a light yellowish-brown powder with good water solubility, and we obtained

a coloured orthodontic adhesives with the ability to easily differentiate it from enamel after incorporating it into the adhesives. This PL-CDs-modified orthodontic adhesives is an important improvement over the ZnQDs-modified orthodontic adhesives by Yan *et al.*[16] The PL-CDs showed a yellowish brown colour without additional UV irradiation, which does not affect the aesthetics of orthodontic treatment, and at the same time helps to accurately remove the orthodontic adhesives during orthodontic treatment and reduces the damage of the enamel in the process of bracket removal.

The PL-CDs modified orthodontic adhesive has important clinical significance, which gives it excellent antibacterial properties and good biocompatibility without affecting its original physical properties. At the same time, its own colour can help orthodontists to accurately remove the adhesive, which is a great progress in the field of modification of orthodontic adhesive, and it has a great advantage over the current modification of orthodontic adhesive. There are also some limitations in this experiment, and the long-term properties of PL-CDs modified orthodontic adhesives in complex oral environments, such as antimicrobial properties and physical properties, still need to be further evaluated for clinical applications.

5. Conclusion

In summary, the adhesive containing 3 wt% of PL-CDs has an efficient antibacterial ability, it has clinically acceptable physicochemical properties and good biocompatibility; it provides desirable anti-demineralisation effects. Based on these, Tb-XT3 provides a new idea to address enamel demineralisation during the fixed orthodontic treatment, and the yellow color visible to the naked eye facilitates the proper removal of residual adhesives, and thus has great value in clinical applications.

Data availability

The data that support the findings of this study are available from the corresponding author upon reasonable request.

Author contributions

Yu Song: resources, funding acquisition, supervision; Yuanping Hao: conceptualization, experimental design and guidance, writing – review & editing; Linlin Xu: writing – original draft, data curation, software, investigation; Qianqian Zhang: writing – review & editing, investigation; Yongzhi Xu: writing – review & editing, investigation; Xuecheng Xu: investigation, supervision; Mingchang Hu and Jidong Xu: software, supervision.

Conflicts of interest

The authors declare no competing financial interest.

Acknowledgements

This work was supported by Supported by Qingdao Key Health Discipline Development Fund(2025–2027), Qingdao Clinical Research Center for Oral Diseases (22-3-7-lczx-7-nsh), Shandong Provincial Key Medical and Health Discipline of Oral Medicine (2025-2027).

References

1 R. Brignardello-Petersen, Orthodontic treatment with fixed appliances may result in small clinical attachment level loss, *J. Am. Dent. Assoc., JADA*, 2018, **149**(4), e70.
2 S. N. Papageorgiou, *et al.*, Treatment outcome with orthodontic aligners and fixed appliances: a systematic review with meta-analyses, *Eur. J. Orthod.*, 2020, **42**(3), 331–343.
3 D. Höchli, *et al.*, Interventions for orthodontically induced white spot lesions: a systematic review and meta-analysis, *Eur. J. Orthod.*, 2017, **39**(2), 122–133.
4 N. Gkantidis, P. Christou and N. Topouzelis, The orthodontic-periodontic interrelationship in integrated treatment challenges: a systematic review, *J. Oral Rehabil.*, 2010, **37**(5), 377–390.
5 K. Srivastava, *et al.*, Risk factors and management of white spot lesions in orthodontics, *J. Orthop. Sci.*, 2013, **2**(2), 43–49.
6 B. S. Lim, *et al.*, Quantitative analysis of adhesion of cariogenic streptococci to orthodontic raw materials, *Am. J. Orthod. Dentofacial Orthop.*, 2008, **133**(6), 882–888.
7 J. Sharan, *et al.*, Applications of Nanomaterials in Dental Science: A Review, *J. Nanosci. Nanotechnol.*, 2017, **17**(4), 2235–2255.
8 M. Behnaz, *et al.*, Shear bond strength and adhesive remnant index of orthodontic brackets bonded to enamel using adhesive systems mixed with TiO2 nanoparticles, *Dent. Press J. Orthod.*, 2018, **23**(4), 43e1–43e7.
9 W. Chaichana, *et al.*, Physical/mechanical and antibacterial properties of orthodontic adhesives containing Sr-bioactive glass nanoparticles, calcium phosphate, and andrographolide, *Sci. Rep.*, 2022, **12**(1), 6635.
10 J. D. Tristán-López, *et al.*, Application of Silver Nanoparticles to Improve the Antibacterial Activity of Orthodontic Adhesives: An *In Vitro* Study, *Int. J. Mol. Sci.*, 2023, **24**(2), 1401.
11 L. Jazi, *et al.*, Evaluation and comparison of the effect of incorporating zinc oxide and titanium dioxide nanoparticles on the bond strength and microleakage of two orthodontic fixed retainer adhesives, *J. World Fed. Orthod.*, 2023, **12**(1), 22–28.
12 N. H. Felemban and M. I. Ebrahim, The influence of adding modified zirconium oxide-titanium dioxide nano-particles on mechanical properties of orthodontic adhesive: an *in vitro* study, *BMC Oral Health*, 2017, **17**(1), 43.
13 J. An, *et al.*, Formulation of arginine-loaded mesoporous silica nanoparticles (Arg@MSNs) modified orthodontic adhesive, *J. Dent.*, 2024, **145**, 104992.
14 A. Sodagar, *et al.*, Evaluation of the antibacterial activity of a conventional orthodontic composite containing silver/hydroxyapatite nanoparticles, *Prog. Orthod.*, 2016, **17**(1), 40.
15 A. Sodagar, *et al.*, Effect of TiO2 nanoparticles incorporation on antibacterial properties and shear bond strength of

dental composite used in Orthodontics, *Dent. Press J. Orthod.*, 2017, **22**(5), 67–74.
16 J. Yan, *et al.*, Multifunctional modification of orthodontic adhesives with ZnO quantum dots, *Dent. Mater.*, 2022, **38**(11), 1728–1741.
17 G. C. Porter, *et al.*, Anti-biofilm activity of silver nanoparticle-containing glass ionomer cements, *Dent. Mater.*, 2020, **36**(8), 1096–1107.
18 Z. T. Hu, *et al.*, An overview of nanomaterial-based novel disinfection technologies for harmful microorganisms: Mechanism, synthesis, devices and application, *Sci. Total Environ.*, 2022, **837**, 155720.
19 G. Dipalma, *et al.*, Nanotechnology and Its Application in Dentistry: A Systematic Review of Recent Advances and Innovations, *J. Clin. Med.*, 2024, **13**(17), 5268.
20 H. S. Budi, *et al.*, Study on the role of nano antibacterial materials in orthodontics (a review), *Braz. J. Biol.*, 2022, **84**, e257070.
21 M. D'Amario, *et al.*, Debonding and Clean-Up in Orthodontics: Evaluation of Different Techniques and Micro-Morphological Aspects of the Enamel Surface, *Dent. J.*, 2020, **8**(2), 58.
22 F. Ahrari, *et al.*, Introducing and assessing the efficacy of a novel method to reduce enamel damage after orthodontic bracket removal using two herbal-based resin colouring agents: An *in vitro* study, *Int. Orthod.*, 2023, **21**(2), 100744.
23 Y. Oweis, *et al.*, Disclosing Agent for Resin Composite Based on Adsorption Surface Treatment, *ACS Appl. Bio Mater.*, 2021, **4**(9), 7222–7233.
24 S. AlSamak, N. R. Alsaleem and M. K. Ahmed, Evaluation of the shear bond strength and adhesive remnant index of color change, fluorescent, and conventional orthodontic adhesives: An *in vitro* study, *Int. Orthod.*, 2023, **21**(1), 100712.
25 C. Lai, *et al.*, An *in vitro* comparison of ultraviolet *versus* white light in the detection of adhesive remnants during orthodontic debonding, *Angle Orthod.*, 2019, **89**(3), 438–445.
26 S. E. Moecke, *et al.*, Efficacy of Bracket Adhesive Remnant Removal by a Fluorescence-Aided Identification Technique with a UV Light Handpiece: *In Vitro* Study, *Int. J. Dent.*, 2022, **2022**, 4821021.
27 Y. F. Huang, *et al.*, One-pot synthesis of highly luminescent carbon quantum dots and their nontoxic ingestion by zebrafish for *in vivo* imaging, *Chemistry*, 2014, **20**(19), 5640–5648.
28 D. He, *et al.*, In vitro and *in vivo* highly effective antibacterial activity of carbon dots-modified TiO(2) nanorod arrays on titanium, *Colloids Surf., B*, 2022, **211**, 112318.
29 M. Havrdova, *et al.*, Toxicity of carbon dots - Effect of surface functionalization on the cell viability, reactive oxygen species generation and cell cycle, *Carbon*, 2016, **99**, 238–248.
30 M. Shamsipur, *et al.*, Facile preparation and characterization of new green emitting carbon dots for sensitive and selective off/on detection of Fe(3+) ion and ascorbic acid in water and urine samples and intracellular imaging in living cells, *Talanta*, 2018, **183**, 122–130.
31 W. B. Zhao, *et al.*, Antibacterial Carbon Dots: Mechanisms, Design, and Applications, *Adv. Healthcare Mater.*, 2023, **12**(23), e2300324.
32 W. Li, *et al.*, Carbon quantum dots enhanced the activity for the hydrogen evolution reaction in ruthenium-based electrocatalysts, *Mater. Chem. Front.*, 2020, **4**(1), 277–284.
33 S. Raina, *et al.*, Bactericidal activity of Cannabis sativa phytochemicals from leaf extract and their derived Carbon Dots and Ag@Carbon Dots, *Mater. Lett.*, 2020, **262**, 127122.
34 S. Pandiyan, *et al.*, Biocompatible Carbon Quantum Dots Derived from Sugarcane Industrial Wastes for Effective Nonlinear Optical Behavior and Antimicrobial Activity Applications, *ACS Omega*, 2020, **5**(47), 30363–30372.
35 X. Yang, *et al.*, A facile injectable carbon dot/oxidative polysaccharide hydrogel with potent self-healing and high antibacterial activity, *Carbohydr. Polym.*, 2021, **251**, 117040.
36 Y. Xu, *et al.*, Poly(Lysine)-Derived Carbon Quantum Dots Conquer Enterococcus faecalis Biofilm-Induced Persistent Endodontic Infections, *Int. J. Nanomed.*, 2024, **19**, 5879–5893.
37 L. M. Baltazar, *et al.*, Antimicrobial photodynamic therapy: an effective alternative approach to control fungal infections, *Front. Microbiol.*, 2015, **6**, 202.
38 M. R. Hamblin, Antimicrobial photodynamic inactivation: a bright new technique to kill resistant microbes, *Curr. Opin. Microbiol.*, 2016, **33**, 67–73.
39 G. Gyulai, *et al.*, Chemical structure and *in vitro* cellular uptake of luminescent carbon quantum dots prepared by solvothermal and microwave assisted techniques, *J. Colloid Interface Sci.*, 2019, **549**, 150–161.
40 H. Li, *et al.*, Degradable Carbon Dots with Broad-Spectrum Antibacterial Activity, *ACS Appl. Mater. Interfaces*, 2018, **10**(32), 26936–26946.
41 H. J. Jian, *et al.*, Super-Cationic Carbon Quantum Dots Synthesized from Spermidine as an Eye Drop Formulation for Topical Treatment of Bacterial Keratitis, *ACS Nano*, 2017, **11**(7), 6703–6716.
42 R. J. Lamont, *et al.*, Salivary-agglutinin-mediated adherence of Streptococcus mutans to early plaque bacteria, *Infect. Immun.*, 1991, **59**(10), 3446–3450.
43 J. M. Tanzer, J. Livingston and A. M. Thompson, The microbiology of primary dental caries in humans, *J. Dent. Educ.*, 2001, **65**(10), 1028–1037.
44 W. Krzyściak, *et al.*, The virulence of Streptococcus mutans and the ability to form biofilms, *Eur. J. Clin. Microbiol. Infect. Dis.*, 2014, **33**(4), 499–515.
45 C. Tuncer, B. B. Tuncer and C. Ulusoy, Effect of fluoride-releasing light-cured resin on shear bond strength of orthodontic brackets, *Am. J. Orthod. Dentofacial Orthop.*, 2009, **135**(1), 14e1–14e6.
46 L. Eslamian, *et al.*, Evaluation of the Shear Bond Strength and Antibacterial Activity of Orthodontic Adhesive Containing Silver Nanoparticle, an In-Vitro Study, *Nanomaterials*, 2020, **10**(8), 1466.
47 H. B. Pont, *et al.*, Loss of surface enamel after bracket debonding: an in-vivo and ex-vivo evaluation, *Am. J. Orthod. Dentofacial Orthop.*, 2010, **138**(4), 387e1–387e9.

48 S. Ryf, *et al.*, Enamel loss and adhesive remnants following bracket removal and various clean-up procedures in vitro, *Eur. J. Orthod.*, 2012, **34**(1), 25–32.
49 A. A. Ribeiro, *et al.*, Assessing adhesive remnant removal and enamel damage with ultraviolet light: An in-vitro study, *Am. J. Orthod. Dentofacial Orthop.*, 2017, **151**(2), 292–296.
50 D. Giugliano, *et al.*, Influence of occlusal characteristics, food intake and oral hygiene habits on dental caries in adolescents: a cross-sectional study, *Eur. J. Paediatr. Dent.*, 2018, **19**(2), 95–100.
51 Y. Chang, L. McLandsborough and D. J. McClements, Antimicrobial delivery systems based on electrostatic complexes of cationic ε-polylysine and anionic gum arabic, *Food Hydrocolloids*, 2014, **35**, 137–143.
52 X. Zhou, *et al.*, Elaboration and characterization of ε-polylysine-sodium alginate nanoparticles for sustained antimicrobial activity, *Int. J. Biol. Macromol.*, 2023, **251**, 126329.
53 R. Ye, *et al.*, Antibacterial activity and mechanism of action of ε-poly-L-lysine, *Biochem. Biophys. Res. Commun.*, 2013, **439**(1), 148–153.
54 Z. Tan, *et al.*, Effects of ε-Poly-l-lysine on the cell wall of Saccharomyces cerevisiae and its involved antimicrobial mechanism, *Int. J. Biol. Macromol.*, 2018, **118**(Pt B), 2230–2236.
55 Y. Qiao, *et al.*, Microwave assisted antibacterial action of Garcinia nanoparticles on Gram-negative bacteria, *Nat. Commun.*, 2022, **13**(1), 2461.
56 A. Anand, *et al.*, Graphene oxide and carbon dots as broad-spectrum antimicrobial agents - a minireview, *Nanoscale Horiz.*, 2019, **4**(1), 117–137.
57 X. Hao, *et al.*, Antibacterial activity of positively charged carbon quantum dots without detectable resistance for wound healing with mixed bacteria infection, *Mater. Sci. Eng. C Mater. Biol. Appl.*, 2021, **123**, 111971.
58 J. C. Kung, *et al.*, Microwave assisted synthesis of negative-charge carbon dots with potential antibacterial activity against multi-drug resistant bacteria, *RSC Adv.*, 2020, **10**(67), 41202–41208.
59 X. Wang, *et al.*, Novel self-etching and antibacterial orthodontic adhesive containing dimethylaminohexadecyl methacrylate to inhibit enamel demineralization, *Dent. Mater. J.*, 2018, **37**(4), 555–561.
60 N. Zhang, *et al.*, Orthodontic cement with protein-repellent and antibacterial properties and the release of calcium and phosphate ions, *J. Dent.*, 2016, **50**, 51–59.
61 L. Wang, *et al.*, Novel bioactive root canal sealer to inhibit endodontic multispecies biofilms with remineralizing calcium phosphate ions, *J. Dent.*, 2017, **60**, 25–35.
62 V. W. Xu, *et al.*, Application of Copper Nanoparticles in Dentistry, *Nanomaterials*, 2022, **12**(5), 889–898.
63 E. Cesur, *et al.*, Effect of different resin removal methods on enamel after metal and ceramic bracket debonding : An *in vitro* micro-computed tomography study, *J. Orofac. Orthop.*, 2022, **83**(3), 157–171.
64 H. J. Joo, *et al.*, Influence of orthodontic adhesives and clean-up procedures on the stain susceptibility of enamel after debonding, *Angle Orthod.*, 2011, **81**(2), 334–340.